P2.16 THE SHONAI AREA RAILROAD WEATHER PROJECT

Scientific objectives and experimental design

Kenichi Kusunoki[1)], Toshiaki Imai[2)], Hiroto Suzuki[3)], Tetsuya Takemi[4)], Kotaro Bessho[1)], Masahisa Nakazato[1)], Wataru Mashiko[1)], Syugo Hayashi[1)], Hanako Inoue[1)], Takaaki Fukuhara[2)], Toru Shibata[2)], Wataru Kato[3)]
1) Meteorological Research Institute, Japan, 2) Railway Technical Research Institute,
3) East Japan Railway Company, and 4) Kyoto University

1. INTRODUCTION

On Japan railroads, wind conditions affect operating efficiency, infrastructure, and safe passage of people and freight. For instance, strong and gusty winds cause regional delays or shutdowns, and especially hazardous crosswinds may lead to overturn of railcars. Since propeller-vane/cup anemometers densely cover on the railroads for operations through some wind speed thresholds (e.g., winds in excess of 25 ms^{-1}), small-scale but strong gusty winds are difficult to detect with the present system. The Shonai area railroad weather project will investigate fine-scale structure of wind gust dynamics and kinetics such as tornadoes, downbursts, and gustfronts.

The ultimate goal of the project is to develop an automatic strong gust detection system for railroads, which the decision to warn is generally based upon information from a single-Doppler radar at low elevation angles. In this presentation, we will introduce an overview of the project as well as highlights from the planned field campaign and some initial results will be presented.

2. THE GOALS OF THE PROJECT

In order to develop an automatic strong gust detection system for railroads using a single-Doppler radar wind observation, the following steps will be implemented (Fig. 1):

Corresponding author address:
* Kenichi Kusunoki, Meteorological Research Institute, 1-1,Nagamine, Tsukuba, Japan
E-mail: kkusunok@mri-jma.go.jp

1) Research on fine-scale structure of strong gust and associated storm dynamics and kinetics.
2) Assessment of radar performance for strong gust detection.
3) Prototype implementation for future strong gust detection system for railroads.

The field campaign and simulations are design to address the above three challenges.

In the first phase of the project (2007-2008), fine-scale structure of strong gusts over the Shonai Plain have been explored using two field campaigns and mesoscale simulations (Table 1). Weather Research and Forecast (WRF) model and the Meteorological Research Institute nonhydrostatic model (MRI-NHM) will be used in this project. The specialized observing platforms have been employed during the field campaign: the MRI X-band portable Doppler radar (X-POD), surface network of automated weather stations, and GPS-sonde soundings launched from the observation vessel. The observation data from these facilities will be combined with data from observing facilities already in place: the JR-East X-band Doppler radar and the wind profiler by the JMA (Japan Meteorological Agency). The field campaign will be described in detail in the next section.

Results from this first phase in the first year will be used to refine observation plans in the second year and assess of Doppler radar performance for strong gust detection during the second phase. At the end of the first phase, the observation and modeling results will be consolidated into an improved understanding of strong gust and associated storm dynamics and kinetics over the Japan Sea side.

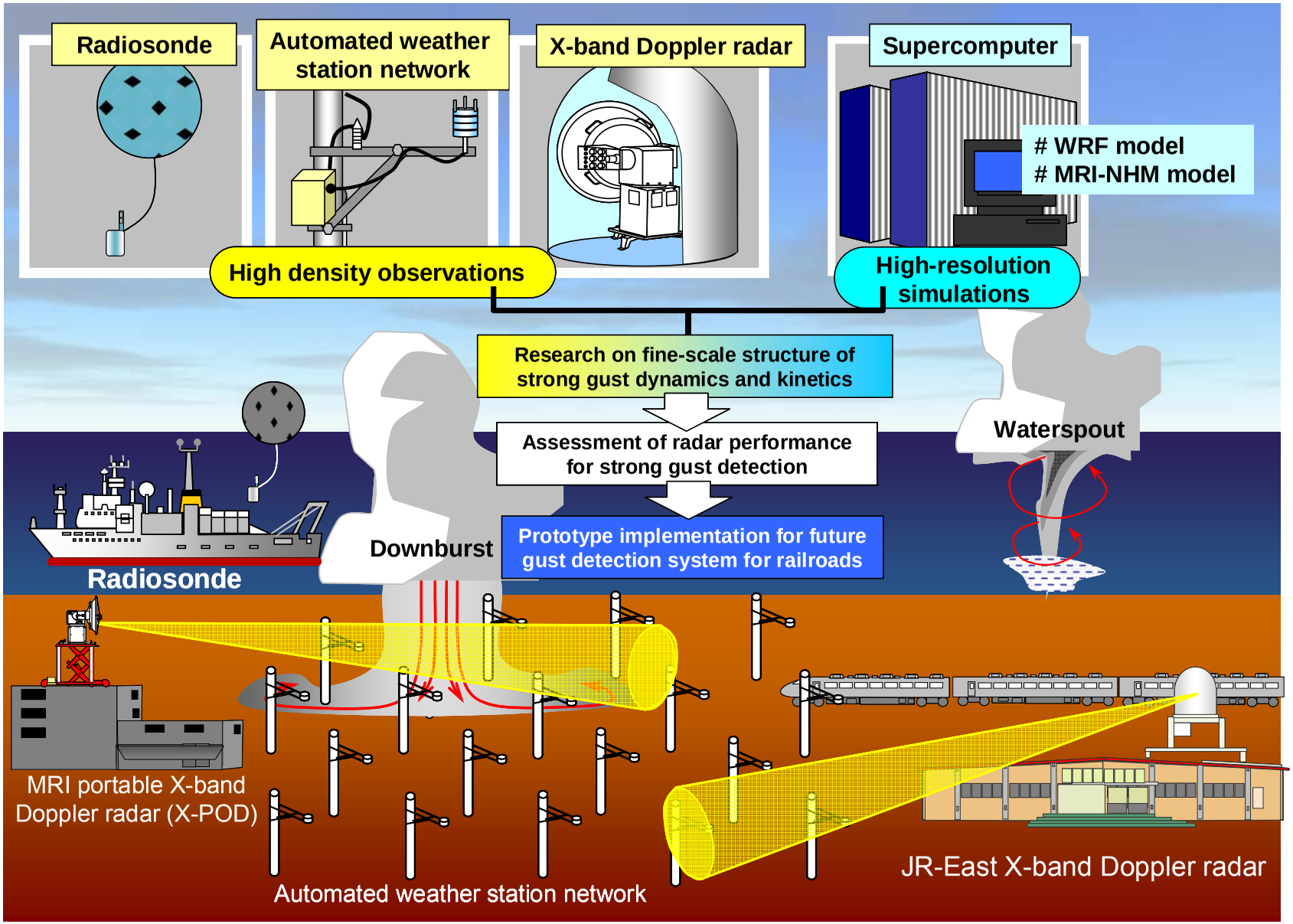

FIG. 1 Block diagram of the project objectives, observing facilities and modeling systems.

3. THE FIELD CAMPAIGN

a. The study area

The high-resolution observations of strong gust phenomena will be performed over the Shonai area (Yamagata Pref., Japan). Primarily, over the Sea of Japan side, severe storms such as tornadoes and gust-generating cold fronts occur frequency in winter season. The Shonai area would provide an ideal setting for studying these phenomena (Fig. 2).

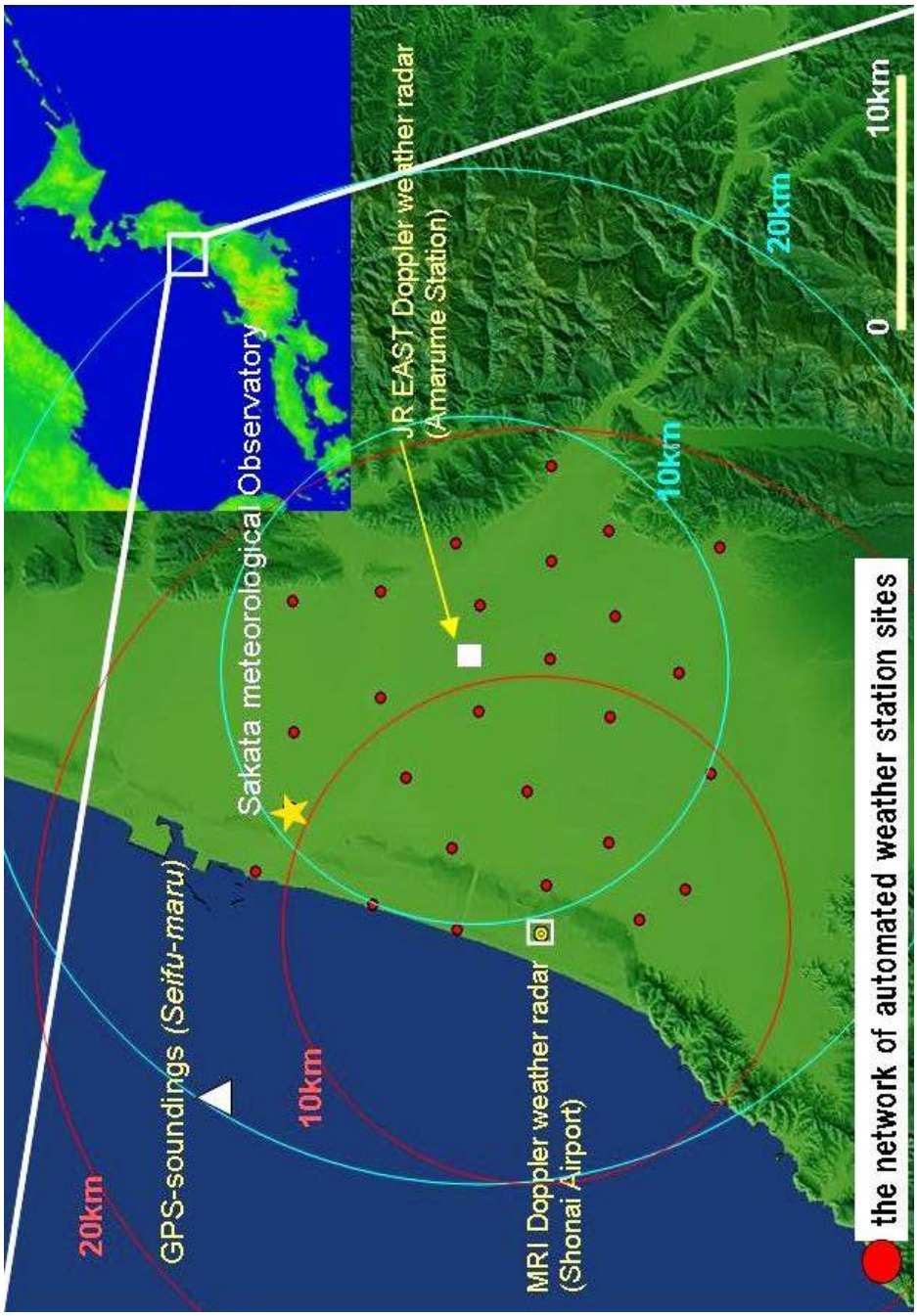

FIG. 2 Map of the Shonai area. The locations marked by the symbols are as follows: the network of automated weather station sites (closed circles), the X-band Doppler radar sites on the Shonai Airport (open square) and on the Amarume Station (closed square), and GPS-sonde soundings will be operated at the research vessel (triangle). The inset shows the locations of the Sea of Japan and the study area (in the square).

System	Organization	Number	Measurements	Observation intervals
MRI X-band Potable Doppler radar (X-POD)	Meteorological Research Institute	1	Radar reflectivity Doppler velocity	3 minutes Volume scan at multiple elevation angles and RHI scans
JR X-band Doppler radar	JR East	1	Radar reflectivity Doppler velocity	30 seconds PPI scan at an elevation angle of 3 degree
Sakata Wind profiler	Japan Meteorological Agency	1	Vertical wind	10 minutes
Surface weater sites	Meteorological Research Institute	26	Surface data	1 second for wind direction and speed 10 seconds for temperature, humidity, pressure, and
Special soundings	Meteorological Research Institute	1	GPS sondes	1-3 hourly
Weather Research and Forecast (WRF) model	Kyoto University	1		
Meteorological Research Institute nonhydrostatic model (MRI-NHM)	Meteorological Research Institute	1		

TABLE 1. Observing facilities and modeling systems.

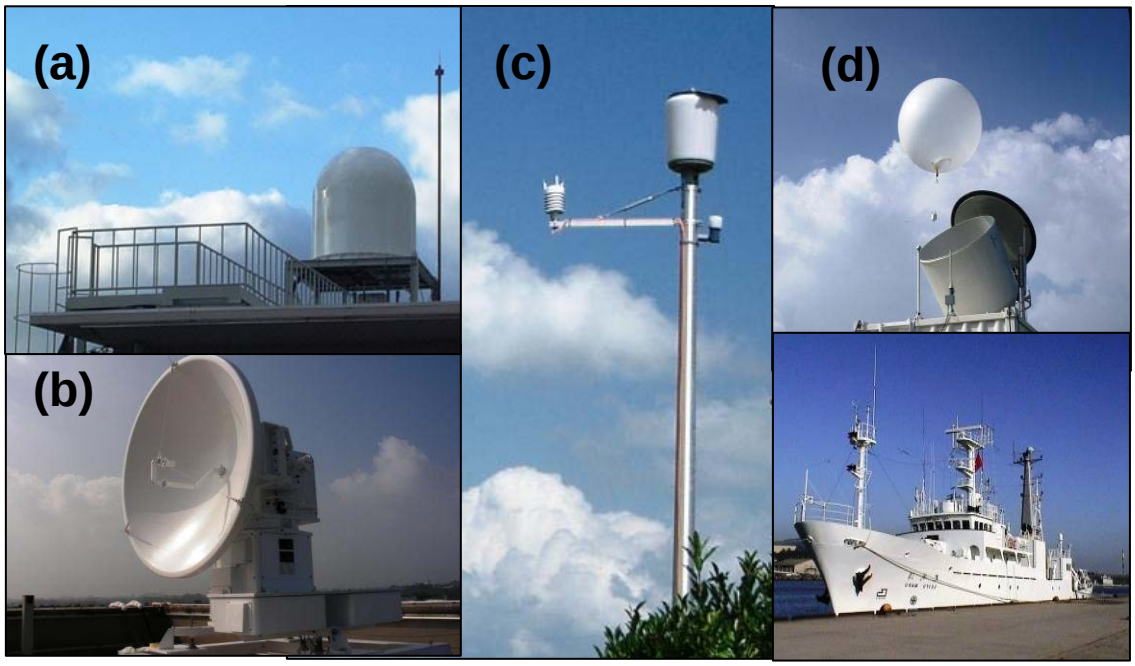

FIG. 3 The primary instruments : (a) JR-East X-band Doppler radar, (b) MRI portable X-band Doppler radar (X-POD), (c) Automated weather station, and (d) GPS-sonde sounding.

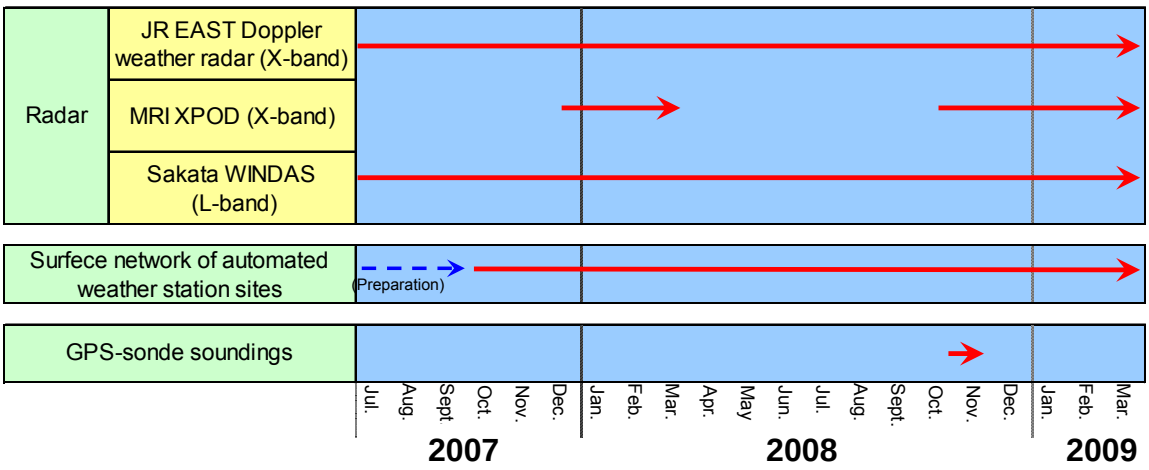

FIG. 4 Timeline for the field campaign.

(a)	**Antenna**	Size	1.2m
		Beamwidth	2.0deg
		Antenna ratation rate	2rpm (single PPII)
	Transmitter	Peak tranmitted power	40kW
		Pulse width	0.2/0.5/1.0μsec
		Range resolution	30/75/150m
		Frequency	9770MHz
		Maximum unambiguous velocity	±27ms-1
		Maximum unambiguous range	30km

(b)	**Antenna**	Size	1.2m
		Beamwidth	2.0deg
		Antenna ratation rate	1-4rpm (multiple PPI + RHI)
	Transmitter	Peak tranmitted power	40kW
		Pulse width	0.2/0.5/1.0μsec
		Range resolution	30/75/150m
		Frequency	9810MHz
		Maximum unambiguous velocity	±27ms-1
		Maximum unambiguous range	60km

Table 2. Characteristics of (a) JR EAST X-band Doppler radar and (b) X-POD.

b. Instrumentations and timeline

Major observing facilities for this project included the two X-band Doppler radar sites, the network of automated weather station sites, and the research vessel capable of releasing soundings (Fig. 3). The timeline for the field campaign is shown in Fig. 4.

1) JR EAST X-band Doppler radar

JR EAST X-band Doppler radar has a 30-km observation range, a 2.0 azimuth resolution, and a pulse length of 1.0 (0.5) micro-sec providing independent data points every 150 (75) m in range. The radar was installed at Amarume station in Shonai Town since March 2007. Since it is needed to observe wind gusts successfully, the radar is operated in a single PPI mode at the lowest elevation angle possible to provide the reflectivity and Doppler velocities as close to the ground. The single elevation angle is 3.0 degree and the scans are taken every 30 s.

2) MRI portable X-band Doppler radar

A portable X-band Doppler radar (X-POD: X-band, POrtable Doppler radar) has been developed as a ground-based radar observation platform to make fine-scale observations of various phenomena. An important aspect of X-POD is its portability. X-POD is basically truck-mounted radar system. X-POD can travel to regions of interesting weather and approach to a range where fine scale measurements. Furthermore, in addition to its small-size and low power consumption, X-POD can be easily dismounted from the truck and deployed on top of a building. The X-POD have been installed on the roof of Shonai Airport building in Sakata City since late December, 2007. The radar, in combination with other devices such as the JR EAST X-band Doppler radar, will be used to obtain detailed meteorological data in the Shonai area. The distance between these radars is 10km and dual-Doppler scanning will be conducted.

The X-POD has a 60-km observation range, a 2.0 azimuth resolution, and a pulse length of 1.0/0.5/0.2 micro-sec providing independent data points every 150/75/30 m in range. It is operated in both PPI and RHI modes (Kusunoki et al. 1996). The key parameters of both radars are summarizes in Table 2.

The X-POD has a 2.5 minute-volume scan update rate with 4-6 constant elevation angles. Furthermore, the X-POD volume scan mode was regularly interrupted by the RHI scans at the azimuth angles of 135 and 315, for observing vertical slices of radar reflectivities and Doppler velocities of storms.

3) Surface network of automated weather station sites

Studies of strong gust and associated small-scale severe local storms can detect from high spatial and temporal resolution observations. In order to characterize and validate the structures near the surface, the surface weather stations were distributed in the study area. We have installed 26 weather transmitter (WXT510; Vaisala) at intervals of 4 kilometers in the area around the Shonai plain. The installation sites are municipally-owned waterworks, farms and parks as well as railway station yards, where each device will be mounted on the top of a steel pole as high as 5 meters. The observation intervals are 1 second for wind direction and wind speed, and 10 seconds for temperature, humidity and pressure. The observation data are to be sent to the computer in the Institute via the Internet. These observations provide a detailed, high quality dataset with which to compare the simulation results. A photograph of the sensor and instrument pole is sown in Fig. 3(c) .

4) GPS-sonde soundings

We are also planning to recognize the vertical structures of strong gust conditions from Vaisala GPS-sonde soundings which will be launched within 1-3 hours interval from the observation vessel *Seifu-maru* located 10 km from the shore in the study area in November 2008.

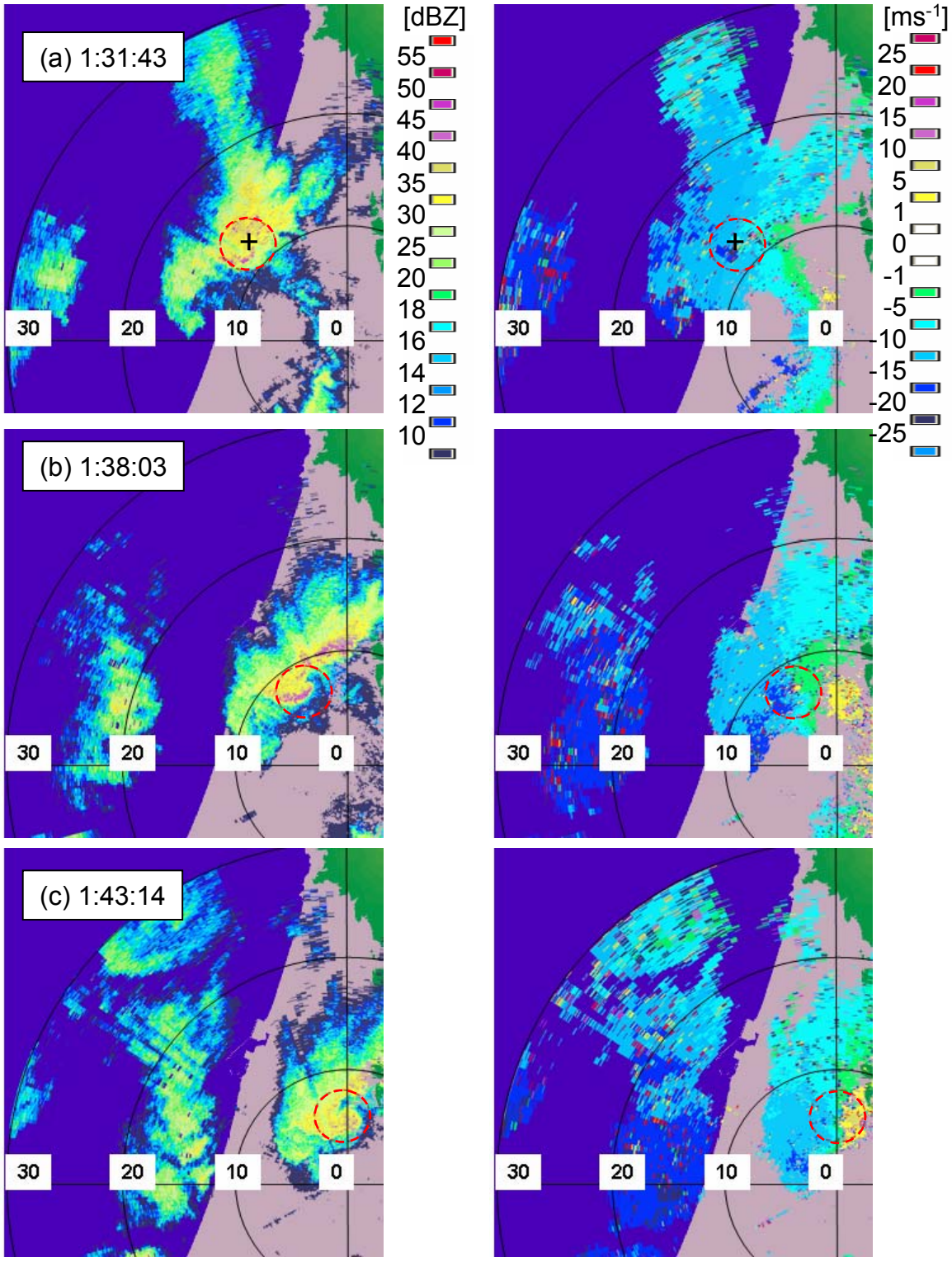

FIG. 5. Radar depiction of a tornadic pattern. Radar reflectivity in dBZ; (right) Doppler velocity in m s-1. Aliasing has not been completely corrected. Color bars are at the right of each panel. Times are shown in local standard time. Range marks are at 10-km intervals centered at the JR-EAST radar. Plus signs in Fig. 5 (a) indicate the position of the automated weather station over which passage of tornadic pattern was identified with the JR-EAST radar.

4. Initial results

On wind gust detection, one of the paramount features is a tornado and/or a larger circulation within which tornadoes are expected to occur. In this section we will briefly present some initial results from the first vortex dataset on 2 December, 2007. The data were basically collected with the JR-EAST Doppler radar. Three automated weather stations were close to the area over which passage of a vortex was identified with the JR-EAST radar. Unfortunately, the surface data was measured at only one station since the other two were faulty. The MRI X-POD had not been installed by 23 December. While some ambiguity remains because there is no direct evidence such as eyewitness of funnel clouds, we believe that the wind gust was associated with a tornado.

a. Synoptic overview

A nearly east-west pressure gradient, which is the typical pattern when the winter monsoon prevails around Japan, appeared between a Siberian high and a cyclone over the Pacific Ocean. The pressure gradient was weak. The storm advected into the radar domain from the Japan Sea and moved eastward through the study area, with wind gust damage reported at the northern part of the City of Sakata.

b. JR-EAST radar

Since the JR-EAST radar performs a single PPI scan every 30 seconds at a low elevation angle only (3.0 degree), a set of scans provided unique datasets to document the temporal as well as spatial variations of the circulation.

The diameter of the reflectivity signature of a hook echo, which is often noted to be associated with tornadoes, was approximately 2km. The height of the radar beam is approximately 260-700m AGL at the range of the hook echo, which may be below cloud base. The circulation may be possible to say it was referred to as a boundary layer misocyclone since its dimension was less than 4 km (Fujita 1981). The location of the counterclockwise curl of the hook echo is consistent with the cyclonic wind field implied by the Doppler velocity data; These velocity pair reveals the flows were far more complicated than those of idealized Rankine vortex; nonetheless, we estimate the cyclonic shear in the Doppler velocity was approximately 20m s^{-1} $(2000m)^{-1}$, that is, approximately $0.01s^{-1}$. The detail quantitative characteristics of the misocyclone will be reported in our upcoming analysis. Note that the reflectivity field reveals that a low reflectivity eye can be seen at the center of the hook echo. Furthermore, the circulation had a spiral structure spiraling outward from the eye. These features which look like hurricanes have been noted previously in radar observations of tornadoes (e.g., Wurman et al. 1996).

c. Wind gust damage survey

The JMA damage survey team investigated locations of the damage path, damage times, and damage magnitude (i.e., F-scale intensity). The vortex trajectory from the JR-EAST radar was consistent with the damage path and damage time. The JMA estimate of the damage was F0 (17-32ms^{-1}). The ground-relative wind speed from the JR-EAST Doppler data was approximately the same magnitude (e.g., 24 ms-1 in the vortex at 1:31JST). If the wind speeds were approximately the same intensity near the surface, the peak wind speed from the Doppler data of higher level of the radar beam would be consistent with the F-scale damage F0. This result will be of major importance for our further investigations concerning wind gust detection algorithm, which is generally based upon a Doppler radar observation.

d. Surface observations

Figure 6 shows the time series of the Surface observations taken at the automated weather station close to the area over which passage of a vortex was identified with the JR-EAST radar. The surface wind speed was relatively weak and the peak was not obvious. The pressure dip and recovery and the wind direction change from 0128 to 0131 JST can be seen. The character of the shift in wind direction is consistent with the theoretical expectation caused by a passage of a counterclockwise circulation.

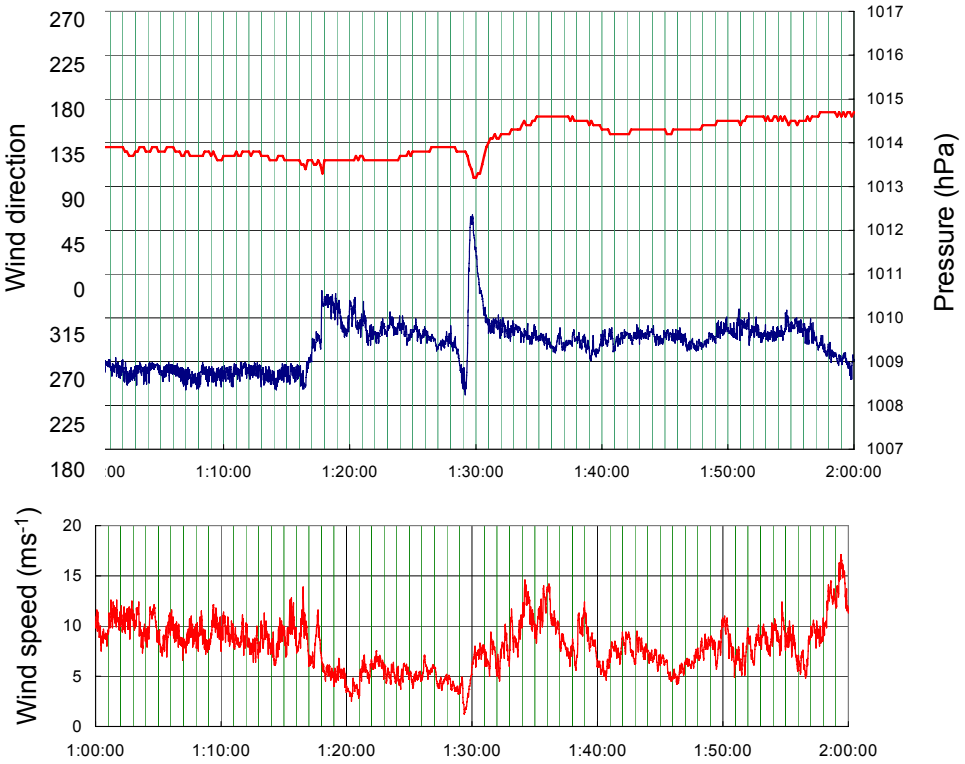

FIG. 6. Surface pressures, surface wind directions, and wind speeds at the automated weather station (the plus sign in Fig. 5(a)).

5. CONCLUSIONS AND FUTURE WORK

In this presentation, we will introduce an overview of the project as well as highlights from the planned field campaign. The preliminary phase of this project, the installation of the network of the surface weather stations, has been completed. The initial results of tornadic echo pattern in this presentation are encouraging. The Doppler radar observations have been applied to more cases than shown in this presentation and are in the process of being further validated by extensive comparison of radar data with surface network data and simulation results.

Acknowledgments. This study was supported by the Program for Promoting Fundamental Transport Technology Research from the Japan Railway Construction, Transport and Technology Agency (JRTT) .

REFERENCES

Fujita, T. T., 1981: Tornadoes and downbursts in the context of generalized planetary scales. *J. Atmos. Sci.,* **38**, 1511-1534.

Kusunoki, K. and T. Ichiyama, 2007: The MRI portable X-band Doppler radar (X-POD): Status and Applications. *Preprints, 33rd Conf. on Radar Meteorology*, Cairns, Australia, Amer. Meteor. Soc. P13A.8.

Kato, W., H. Suzuki, M. Shimamura, K. Kusunoki, and T. Hayashi, 2007: The design and initial testing of an X-band Doppler radar for monitoring hazardous winds for railroad system. Preprints, *33rd Conf. on Radar Meteorology*, Cairns, Australia, Amer. Meteor. Soc. P13A.15.

Wurman, J., J. M. Straka, and E. N. Rasmussen, 1996: Fine-scale Doppler radar observations of tornadoes. *Science*, **272**, 1774-1777.